



Niobium promotes fracture healing in rats by regulating the PI3K-Akt signalling pathway: An *in vivo* and *in vitro* study



Jia Tan^{a,c}, Jiabin Li^b, Bojun Cao^{a,c}, Junxiang Wu^{a,c}, Dinghao Luo^{a,c}, Zhaoyang Ran^{a,c}, Liang Deng^{a,c}, Xiaoping Li^d, Wenbo Jiang^c, Kai Xie^{a,c,**}, Lei Wang^{a,c,***}, Yongqiang Hao^{a,c,*}

^a Shanghai Key Laboratory of Orthopaedic Implants Department of Orthopaedic Surgery, Shanghai Ninth People's Hospital, Shanghai Jiao Tong University School of Medicine, Shanghai, 200011, China

^b Department of Orthopedics, The Second Affiliated Hospital of Harbin Medical University, Harbin, 150001, China

^c Clinical and Translational Research Center for 3D Printing Technology, Shanghai Ninth People's Hospital, Shanghai Jiao Tong University School of Medicine, Jin Zun Road No. 115, 200011, Shanghai, China

^d Ningxia Orient Ta Ind Co, 119, Yejin Road, Dawukou District, Shizuishan, Ningxia, 753000, PR China

ARTICLE INFO

Keywords:

Fracture healing
Niobium
Orthopaedic implant
PI3K-Akt pathway

ABSTRACT

Background: Stable fixation is crucial in fracture treatment. Currently, optimal fracture fixation devices with osteoinductivity, mechanical compatibility, and corrosion resistance are urgently needed for clinical practice. Niobium (Nb), whose mechanical properties are similar to those of bone tissue, has excellent biocompatibility and corrosion resistance, so it has the potential to be the most appropriate fixation material for internal fracture treatment. However, not much attention has been paid to the use of Nb in the area of clinical implants. Yet its role and mechanism of promoting fracture healing remain unclear. Hence, this study aims at elucidating on the effectiveness of Nb by systematically evaluating its osteogenic performance via *in vivo* and *ex vivo* tests.

Methods: Systematic *in vivo* and *in vitro* experiments were conducted to evaluate the osteogenic properties of Nb. *In vitro* experiments, the biocompatibility and osteopromoting activity of Nb were assessed. And the osteoinductive activity of Nb was assessed by alizarin red, ALP staining and PCR test. *In vivo* experiments, the effectiveness and biosafety of Nb in promoting fracture healing were evaluated using a rat femoral fracture model. Through the analysis of gene sequencing results of bone scab tissues, the upregulation of PI3K-Akt pathway expression was detected and it was verified by histochemical staining and WB experiments.

Results: Experiments in this study had proved that Nb had excellent *in-vitro* cell adhesion and proliferation-promoting effects without cytotoxicity. In addition, ALP activity, alizarin red staining and semi-quantitative analysis in the Nb group had indicated its profound impact on enhancing osteogenic differentiation of MC3T3-E1 cells. We also found that the use of Nb implants can accelerate fracture healing compared to that with Ti6Al4V using an animal model of femur fracture in rats, and the biosafety of Nb was confirmed *in vivo* via histological evaluation. Furthermore, we found that the osteogenic effects of Nb were achieved through activation of the PIK/Akt3 signalling pathway.

Conclusion: As is shown in the present research, Nb possessed excellent biosafety in clinical implants and accelerated fracture healing by activating the PI3K-Akt signalling pathway, which had good prospects for clinical translation, and it can replace titanium alloy as a material for new functional implants.

* Corresponding author. Shanghai Key Laboratory of Orthopaedic Implants Department of Orthopaedic Surgery, Shanghai Ninth People's Hospital, Shanghai Jiao Tong University School of Medicine, Shanghai, 200011, China.

** Corresponding author. Shanghai Key Laboratory of Orthopaedic Implants Department of Orthopaedic Surgery, Shanghai Ninth People's Hospital, Shanghai Jiao Tong University School of Medicine, Shanghai, 200011, China.

*** Corresponding author. Shanghai Key Laboratory of Orthopaedic Implants Department of Orthopaedic Surgery, Shanghai Ninth People's Hospital, Shanghai Jiao Tong University School of Medicine, Shanghai, 200011, China.

E-mail addresses: kai.xie@hotmail.com (K. Xie), wanglei12041985@163.com (L. Wang), hyq_9hospital@hotmail.com (Y. Hao).

<https://doi.org/10.1016/j.jot.2022.08.007>

Received 25 April 2022; Received in revised form 18 July 2022; Accepted 18 August 2022

1. Introduction

Fractures, a common clinical condition, account for 16% of all musculoskeletal injuries [1]. There has been a dramatic rise in traumatic and life-threatening long bone fractures in recent years due to the increasing access to motorized transport throughout the developing world as well as the increase in natural disasters and industrial accidents [2]. As a good fracture fixation lies the foundation of fracture treatment, it leads to a surge in the demand for required internal and external fixation devices for such treatment. In 2013, the global market for the fixation devices was valued at \$5.7 billion and is growing at a rate of 7.2% [3]. Early treatment, anatomic repositioning, and rigid fixation are primary treatments of fractures while surgical treatments are required in open fractures, closed fractures with failed manipulative reduction, and old fractures with suboptimal function. Internal fixation devices such as screws, intramedullary nails, and steel plates are generally applied in such treatments.

Among the clinical internal fixation devices, titanium (Ti) implants are widely used owing to their good mechanical properties and biocompatibility [4]. Nevertheless, these rigid bone implant materials still have the following insurmountable disadvantages except for its excellent mechanical and corrosion resistance properties: 1) the lack of biological activity, poor osteoconductivity, and difficulty in promoting fracture repair by regulating osteoblast and osteoclast functions; 2) possibility to cause metallic artefacts when performing CT and MRI examinations with stainless steel and Ti-based implants, which might affect the clinician's observation of the lesion [5]. Poor healing which has great clinical significance and socioeconomic effects, resulting in an average economic loss of more than \$10,000 per non-healing fracture [6]. complications that further exacerbates the pain and financial burden of the fracture patients. Hence, it is of great clinical value and social significance to overcome the inherent defects of existing orthopaedic implants and develop a class of internal fixation materials with better mechanical properties and good osteoinductivity.

Recently, a new generation of metallic biomaterials based on expensive refractory elements of the IVB and VB groups with good wear resistance, such as tantalum (Ta), zirconium (Zr), and niobium (Nb), has attracted tremendous attention. Nb is an off-white metal with an atomic number of 41 and an atomic weight of 92.9. If Nb is to be used as a material for orthopaedic implants, its biomechanical properties should be a primary requirement. Clinically, the elastic modulus mismatch between the implant and the surrounding bone tissue has been identified as a major cause of pain during walking, stress shielding, implant loosening, and even bone resorption [7,8]. Furthermore, the mismatch in modulus can lead to excessive micromotion between the implant and bone, which prevents bone formation and instead promotes the inward growth of fibrous tissue, leading to the impediment of the implant osseointegration.

Compared to Ti6Al4V (elasticity modulus of approximately 114 GPa) [8], Nb has an elasticity modulus of 108 GPa [9], which provides sufficient mechanical fixation and support to facilitate fracture repair during fracture healing. In addition to its good radiopacity for CT and MRI examinations, Nb has low MRI compatibility (overall magnetisation, stainless steel: $3520\text{--}6700 \times 10^6$; Nb: 237×10^6) [10], which can greatly reduce the negative effects of metallic artefacts during the physicians' interpretation of x-ray films. As is shown in previous studies, Nb has been investigated and used as an implantable material due to its excellent biocompatibility, mechanical and corrosion resistance, and osteoconductivity [11]. Nb metal implanted in soft and hard tissues of rats both showed good biocompatibility and osteogenic effects [9]. *In vitro* apatite formation assays and *in vivo* histomorphometric studies indicate that Nb metal is biologically active and can be biologically bound to bone [12]. It is demonstrated in a study that the formation of a protective oxide layer on its surface attributes to the excellent biocompatibility, corrosion resistance and the osteoconductivity of the Nb metal [13]. Moreover, such oxide coatings of Nb, which promote cellular metabolic activity, increases cell viability, and collagen I production, have been shown to

facilitate cell proliferation that can reduce the negative effects of metallic artifacts during the physician's review process [14]. Nb₂O₅ coatings improve the surface properties of stainless steel (e.g. hardness, corrosion resistance, and bioreactivity) [15] and it also promotes adhesion, proliferation, and osteogenic differentiation of rat bone mesenchymal stem cells [16]. Although previous literature has already clarified the excellence of Nb's biocompatibility, *in vivo* studies on the use of Nb for fracture healing are still lacking, and the mechanisms by which Nb metals promote fracture healing have not been clarified.

Based on the above observations, we made a hypothesis that Nb has a facilitative effect on fracture healing. We proposed to evaluate the osteogenic effects, biocompatibility, and biosafety of Nb metal implants *in vitro* and *in vivo* in the present study. Nb metal was utilized as an intramedullary nail to study its effect on fracture healing in a rat femur fracture model and was compared with that of Ti6Al4V in the study. In addition, the effect of Nb metal implants on fracture healing was also determined by assessing the fracture repair healing and performing histological assessments, attempting to explore its major signalling pathways and determine its *in vitro* cytocompatibility and *in vivo* biosafety.

2. Materials and methods

2.1. *In vitro* cytocompatibility and osteogenic differentiation

2.1.1. Cell proliferation and morphology

MC3T3-E1 cells were seeded on the surface of the discs (diameter*height: 10 × 2 mm) in 24-well plates at a density of 5×10^4 /well, and cells were incubated in α -MEM with 10% foetal bovine serum at 37 °C with 5% CO₂. Cell proliferation was examined at the 1, 3, 5, and 7 days after the co-culture with the material respectively (n = 5). Cell viability was measured using the Cell Counting Kit-8 (CCK-8; Dojindo Molecular Technology, Japan). The reagent was added to the wells at a ratio of 1:10 and then incubated for 2 h. Optical density (OD) was tested at 405 nm using an ELX800 microplate reader (Bio-Tek, USA). MC3T3-E1 cells were inoculated at a density of 5×10^4 /well on the surface of the material in 24-well plates (n = 5). After the α -MEM medium was discarded, each sample was washed three times with PBS and fixed overnight at 4 °C in 2.5% glutaraldehyde solution, then subjected to dehydration in gradient alcohol solutions (50, 60, 70, 80, 90, and 100%) for 15 min each. After dehydration, each sample was dried at 37 °C. Cell morphology was observed through scanning electron microscopy (SEM, S-4800; Hitachi, Japan). Additionally, each sample was washed three times with PBS and then fixed in 4% paraformaldehyde solution for 30 min at room temperature. Thereafter, each sample was stained with phalloidin for 30 min at room temperature for cytoskeletal staining, and nuclei were counterstained with 4',6 diamidino-2-phenylindole (Sigma, D9542-10 MG, DAPI) for 15 min. Images were taken by fluorescence microscopy (Leica Microsystems, Heidelberg, Germany).

2.1.2. LIVE/DEAD staining

Cells (5×10^4 /well for MC3T3-E1 cells) were inoculated in a 24-well plate with the material and corresponding medium (n = 5). After 24 h of incubation, the medium was gently removed. Cells were stained with the Calcein-AM/PI Double Staining Kit (Dojindo Molecular Technology, Japan) at room temperature.

2.1.3. Osteogenic differentiation

Alkaline phosphatase (ALP) activity is an early marker of osteoblast differentiation, through which the osteogenic differentiation of MC3T3-E1 cells was assessed along with alizarin red staining. MC3T3-E1 cells (5×10^4 /well) were inoculated on Ti₆Al₄V and Nb discs, and after 3 days (n = 5), when the cells were fully attached to the scaffold, the growth medium was discarded and replaced with osteogenic differentiation medium (HUXMA-90021, Cyagen, USA), which was then replaced every 3 days. Cells cultured in osteogenic differentiation medium for 7 days were used to measure the activity of ALP using activity assay kit (P0321;

Beyotime, China) according to the manufacturer's instructions. First, the medium was carefully removed, and the material was washed three times with PBS. Next, 0.2% triton X-100 solution was added. The substrate and p-nitrophenol were then added and incubated at 37 °C for 10 min and ALP activity was measured at 405 nm.

After 21 days of incubation, the material was then transferred to a new 24-well cell culture plate, washed three times with PBS, and fixed in 4% paraformaldehyde for 30 min at room temperature. After alizarin red staining, the material was washed with PBS solution until the solution was clear. Thereafter, the stained mineralised nodules were dissolved with 10% cetylpyridinium chloride (C9002-25G; Sigma, USA) and assayed semi-quantitatively by measuring the absorbance at 562 nm.

2.2. Quantitative real-time polymerase chain reaction (RT-PCR)

MC3T3-E1 cells were inoculated at a density of 5×10^4 /well in a 24-well culture plates (n = 5). After cells were fully adherent, the α -MEM complete medium was replaced with osteogenic induction medium (complete medium with ascorbic acid, dexamethasone, and β -glycerophosphate), and the medium was changed every 2 days. Osteogenesis-related genes were detected after 7 days of co-culture with the scaffold, and osteopontin (OPN), osteocalcin (OCN), ALP, type 1 collagen (Col-1), and runt-related transcription factor-2 (Runx2) expression was examined to detect the osteogenic differentiation of MC3T3-E1 cells. Total RNA from MC3T3-E1 cells co-cultured with the material was extracted using TRIzol; then, reverse transcription was performed to obtain cDNA via PrimeScript RT Master Mix (Takara). RT-PCR reactions were performed by SYBR Premix Ex TaqII (Takara) on a CFX96 PCR system (Bio-Rad). The housekeeping gene GAPDH was used as a control. The primers used are provided in Table S1.

2.3. Animals and surgical procedures

Animal experiments conformed to the Chinese Animal Experimentation Law and were approved by the ethics committee of Shanghai Jiao Tong University School of Medicine (ethical number: SH9H-2022-A785-SB). A total of 72 8-week-old male Sprague–Dawley rats (Shanghai Sipper BK Laboratory Animals Ltd) randomly divided into 6 groups (n = 12). All rats were housed in a barrier facility under high-efficiency particulate air filtration and allowed *ad libitum* access to water and standard laboratory pellets. Anaesthesia was induced via the abdominal injection of pentobarbital sodium. The surgical site was shaved and disinfected, and a 2 cm incision was made on the lateral side of the right hind leg to access the skin and fascial layers to expose the quadriceps muscle and bluntly separate it to reveal the femur. A lateral osteotomy was performed at the mid-femur by sawing, and tissues of the two groups of animals were fixed using Nb rods 3.5 cm in length and 1.5 mm in diameter, as well as Ti6Al4V rods as intramedullary nails. The incisions were sutured layer-by-layer and disinfected again. The right femur was injected subcutaneously with 20 mg/kg of sterile calcein solution 7 and 14 days before sampling. Sampling was performed after euthanasia at 4, 8, and 12 weeks after surgery.

2.4. Medical imageology evaluation

Frontal and lateral slices of the right femur were assessed through a Faxitron MultiFocus X-ray system (Faxitron, Bioptrics, LLC, USA) for small animals according to the manufacturer's instructions. After fixation in 4% paraformaldehyde for 72 h, femoral specimens were stored in 70% ethanol for micro-CT scanning (μ CT 80; SCANCO Medical AG, Bassersdorf, Switzerland) (n = 3). The middle femur was considered the region of interest. The bone folding line is centered on 200 layers above and below, with a layer thickness of 18 microns. A high-resolution 3D reconstruction of the mid-femur was also performed. Bone volume/tissue volume (BV/TV), mean trabecular thickness (Tb.Th), mean trabecular spacing (Tb.Sp), and number of trabeculae (Tb.N) were quantified. We

determine the success of fracture healing by the results of X-ray and micro-CT.

2.5. Histological analysis

After micro-CT analysis, the samples were embedded in methyl methacrylate. Hard tissue sections were generated from the embedded specimens via the Cut and Grind System (Buehler 11-1280-250, USA) system. Tissue sections were stained with van Gieson's picrofuchsin (n = 3). Images were captured with a Nikon SMZ 1500 stereomicroscope (Nikon Instruments, Melville, NY). Femoral specimens were fixed in 4% paraformaldehyde for 72 h and decalcified with ethylenediaminetetraacetic acid. After dehydration, all decalcified femoral specimens were embedded in paraffin. Samples were section and stained with haematoxylin-eosin (HE), Movat and immunohistochemical reagents for PI3K and Akt (n = 5).

2.6. Transcriptomic analysis

The effects of Nb on fracture healing and associated mechanisms were investigated via transcriptomic analysis. After euthanising experimental animals at 8 weeks post-surgery, the right hind leg mid-femoral callus was removed under aseptic conditions and fragmented for storage in liquid nitrogen; the total RNA was then isolated and extracted. Transcriptomic analysis was performed by Applied Protein Technology Co. Ltd. Differential expression analysis was performed using the DESeq2 R package (1.16.1). Gene ontology (GO) and Kyoto Encyclopedia of Genes and Genomes (KEGG) enrichment analyses were performed to determine the potential biological functions of differentially expressed genes.

2.7. Western blot analysis

After 7 and 14 days of co-culture with the material (n = 5), the cells were lysed with RIPA lysis buffer (P0013K, Beyotime, China) on ice for 30 min. The proteins were then scraped off and transferred to centrifuge tubes for centrifugation. The protein concentration was measured by colorimetry (Thermo Scientific, MA) after centrifugation. Then, the loading buffer (P0015, Beyotime, China) was added to the centrifuge tube, which was boiled for 10 min at 100 °C. Twenty micrograms of protein was added to the lane for electrophoresis and then transferred to a polyvinylidene fluoride membrane (IPVH00010, Millipore, USA). The membranes were then incubated with 5% skim milk. Primary antibodies against Akt (4691L, Cell Signaling, China), PI3K (ab227204, Abcam, U.K.), Col-1 (14695-1-AP, Proteintech, China), OCN (ab93876, Abcam, U.K.), ALP (ab108337, Abcam, U.K.) and OPN (22952-1-AP, Proteintech, China) were incubated with the blots overnight at 4 °C. The membranes were washed three times with PBS and then incubated with secondary antibodies at room temperature for 2 h. To visualise the bands, a chemiluminescence kit (Thermo Scientific, MA) was used.

2.8. Statistical analysis

The sample size for this study was 3 unless otherwise stated. Data are expressed as mean \pm standard deviation. A Student's t-test and one-way analysis of variance were used to determine the variance using SPSS version 23.0 software (IBM Corp.). A difference of $P < 0.05$ was considered to be significant.

3. Results

3.1. Material characterisation

The morphology of the Nb and Ti6Al4V discs was determined by a SEM (Fig. 1).

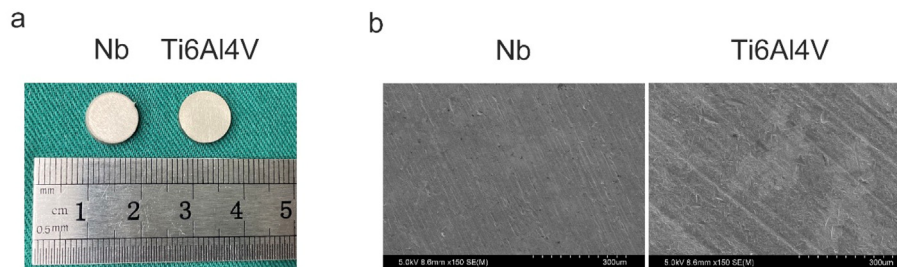


Figure 1. (a) Niobium (Nb) and Ti6Al4V discs (diameter*height: 10 × 2 mm) used for *in vitro* experiments. (b) Scanning electron microscopy (SEM) micrograph of the blank sample of the discs.

3.2. Cell proliferation and adhesion

The morphology of MC3T3-E1 cells cultured on both material discs for 7 days was observed by SEM (Fig. 2a). Cells could be detected on all discs examined. Cells on the discs in the Nb group spread well and showed extended cell pseudopodia. To investigate cell adhesion, we performed fluorescent staining of MC3T3-E1 cells (Fig. 2b). DAPI and phalloidin staining showed higher cell adhesion on the Nb group discs than that of the Ti6Al4V group, and the cells in the Nb group spread more than those in the Ti6Al4V group. The proliferation of cells inoculated on the scaffolds was assessed using the CCK-8 assay (Fig. 2c), which showed that the number of cells in the Nb and Ti6Al4V groups grew with increasing incubation duration. This result indicated that Nb has good *in vitro* cytocompatibility, and the cell count in the Nb group was essentially the same as that in the blank control group, indicating that Nb is non-toxic to MC3T3-E1 cells.

3.3. LIVE/DEAD staining

The results of live-dead staining indicated that there was no increase in the number of dead cells in the Nb group compared with that in the Ti6Al4V group, which are consistent to results above; it also showed that cells in the Nb group were fuller and rounder than those in the Ti6Al4V group (Fig. 2d).

3.4. Osteogenic differentiation

To determine the potential osteogenic effect, MC3T3-E1 cells were cultured in sample extracts supplemented with ascorbic acid, β -glycerophosphate, and dexamethasone. The osteogenic differentiation effect of Nb and Ti6Al4V on MC3T3-E1 cells was determined by ALP and alizarin red staining. The ALP activity of both groups was tested on day 7, and the result in the Nb group was higher than that in the Ti6Al4V group (Fig. 3a), indicating that Nb enhanced the osteogenic differentiation of MC3T3-E1 cells at an early stage compared to that with Ti6Al4V. In addition, alizarin red staining (Fig. 3b) and semi-quantitative analysis (Fig. 3c) on day 21 showed that calcium nodules were formed on the material in all groups, and there were significantly more calcium nodules in the Nb group than in the Ti6Al4V alloy group, indicating that Nb has potential osteogenic properties.

3.5. RT-PCR

Osteogenic differentiation was assessed by quantitative RT-PCR analysis of expression of the osteogenic markers *OPN*, *OCN*, *ALP*, *Col-1*, and *Runx2* at days 7 and 14. Levels of *Col-1*, *ALP*, and *Runx2* were higher in the Nb group than in the Ti6Al4V group at both time points (Fig. 3d, e, h). In contrast, *OCN* and *OPN* expression levels did not differ between the groups at day 7 but were significantly higher in the Nb group at day 14 (Fig. 3f and g). These results suggest that Nb exhibits superior osteogenic differentiation of MC3T3-E1 cells.

3.6. Radiographic evaluation

Post-operative X-rays showed that all intermedullary nails were inserted in the femur medulla and no displacement of intermedullary nails was observed 4, 8, and 12 weeks after surgery. X-ray and micro-CT analyses were used to monitor post-operative new bone formation. X-ray results showed that fracture lines were visible in both groups at week 4, with more high-density bone formation around the fracture line in the Nb group than in the Ti6Al4V group (Fig. 4a). At week 8, there was significant callus formation around the fracture end in both groups and there were outstandingly more bridging calluses around the fracture at weeks 4 and 8 in the Nb group than in the Ti6Al4V group. The formation of the continuous callus was nearly complete at 8 weeks post-fracture in the Nb group, whereas it was delayed to 12 weeks in the Ti6Al4V groups. At week 12, the callus around the end of the fractured femur in the Nb group was remarkably calcified into the woven bone, indicating a further increase in local bone density at the end of the segment. In addition, the fracture line in the Nb group almost disappeared and callus remodelling was notably better than that in the Ti6Al4V group. In addition, to closely observe the fracture healing process, micro-CT was utilized to examine the samples. The 3D reconstructed micro-CT and cross-sectional images (Fig. 4b) showed that the callus in the Nb group was larger at 4 weeks after surgery compared with that in the Ti6Al4V group. At weeks 8 and 12, the cross-sectional images showed that the callus in the steel and Nb groups had gradually started to shrink and calcify into lamellar bone after remodelling, whereas the Ti6Al4V group still showed larger callus tissue. Compared with Ti6Al4V group, the BV/TV values of the Nb group at each time point were higher. The Nb group also had the higher Tb.N and Tb.Th and the lower Tb.Sp of the two groups at week 12 (Fig. 4d,e,f). Overall, it could be inferred that Nb not only promoted osteogenesis in the callus but also upregulated the efficiency of callus remodelling.

3.7. Histological evaluation

HE staining showed the general evolution of the bone callus tissue (Fig. 5a). At week 4, the callus in the Ti6Al4V group consisted mainly of fibrous components, whereas the Nb group appeared to have more calcified tissue. At week 8, the fibrous healing tissue around the fracture end of the femur was completely calcified into woven bone in the Nb group, and remodelling and consolidation of the calcified callus occurred. Remodelling of the callus tissue was better in the Nb group by week 12. Van Gieson-stained images of both groups at each time point (weeks 4, 8, 12) are shown in Fig. 5b, with a larger area of new bone in the Nb group at week 8 compared with that in the Ti6Al4V group and lower than that in the Ti6Al4V group at week 12. Movat staining (Fig. 5c) showed that the Nb group had more cartilage calcification at the fracture site at week 4, which had completely calcified into woven bone at week 8, whereas the Ti6Al4V group showed more cartilage calcification only at week 8. These results suggested that Nb can accelerate the formation of new bone. During fracture healing, new bone formation and bone reconstruction can be assessed via continuous fluorescent labelling using

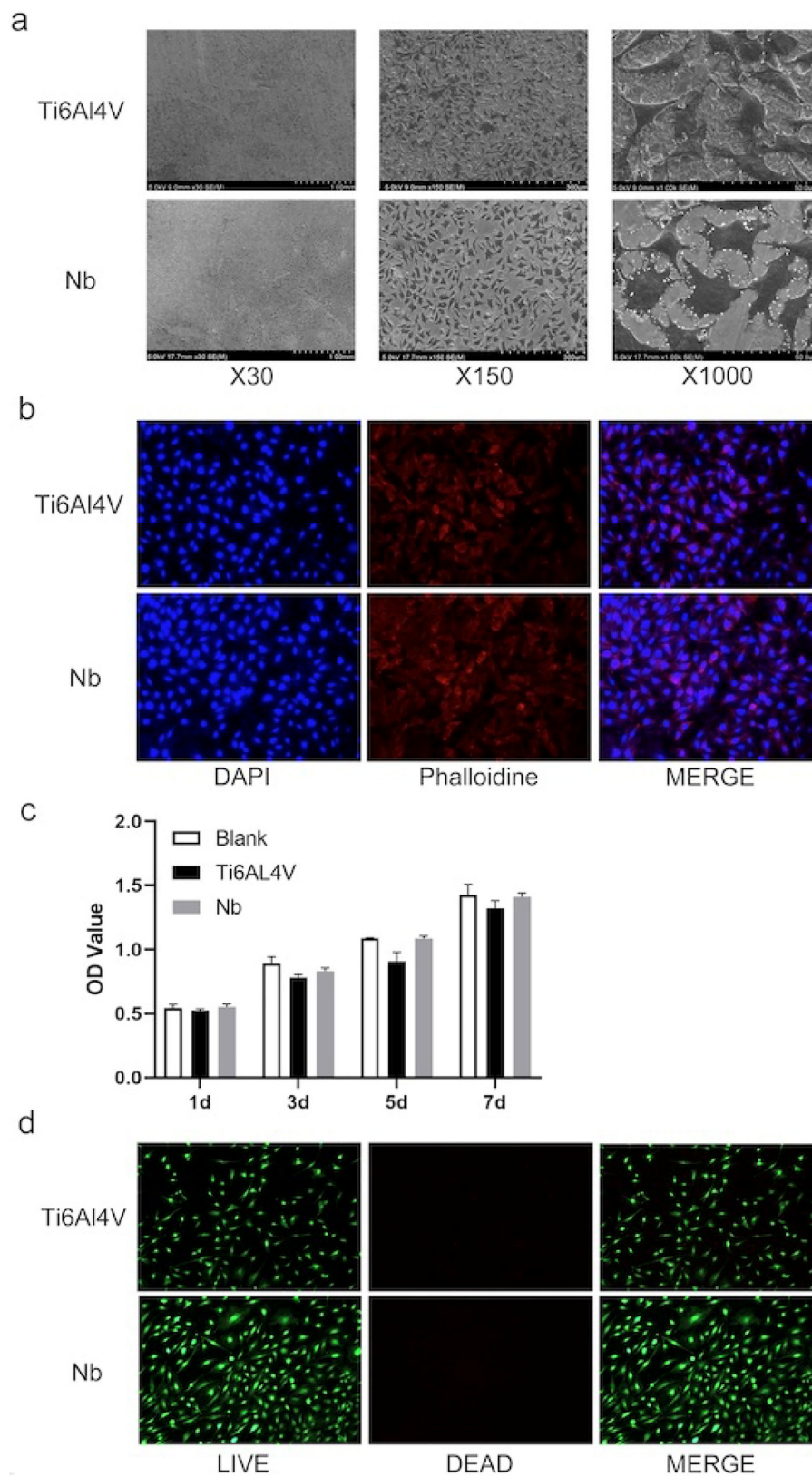


Figure 2. (a) Scanning electron microscopy (SEM) micrographs showing MC3T3-E1 cells adhering to niobium (Nb) and Ti6Al4V discs. (b) Fluorescent labelling of MC3T3-E1 cells adhering to the discs with DAPI and phalloidin. (c) Cell growth on niobium (Nb) and Ti6Al4V discs, with higher optical density (OD) values indicating more cell growth in the Nb group. (d) Live-dead staining of MC3T3-E1 cells adhering to the discs.

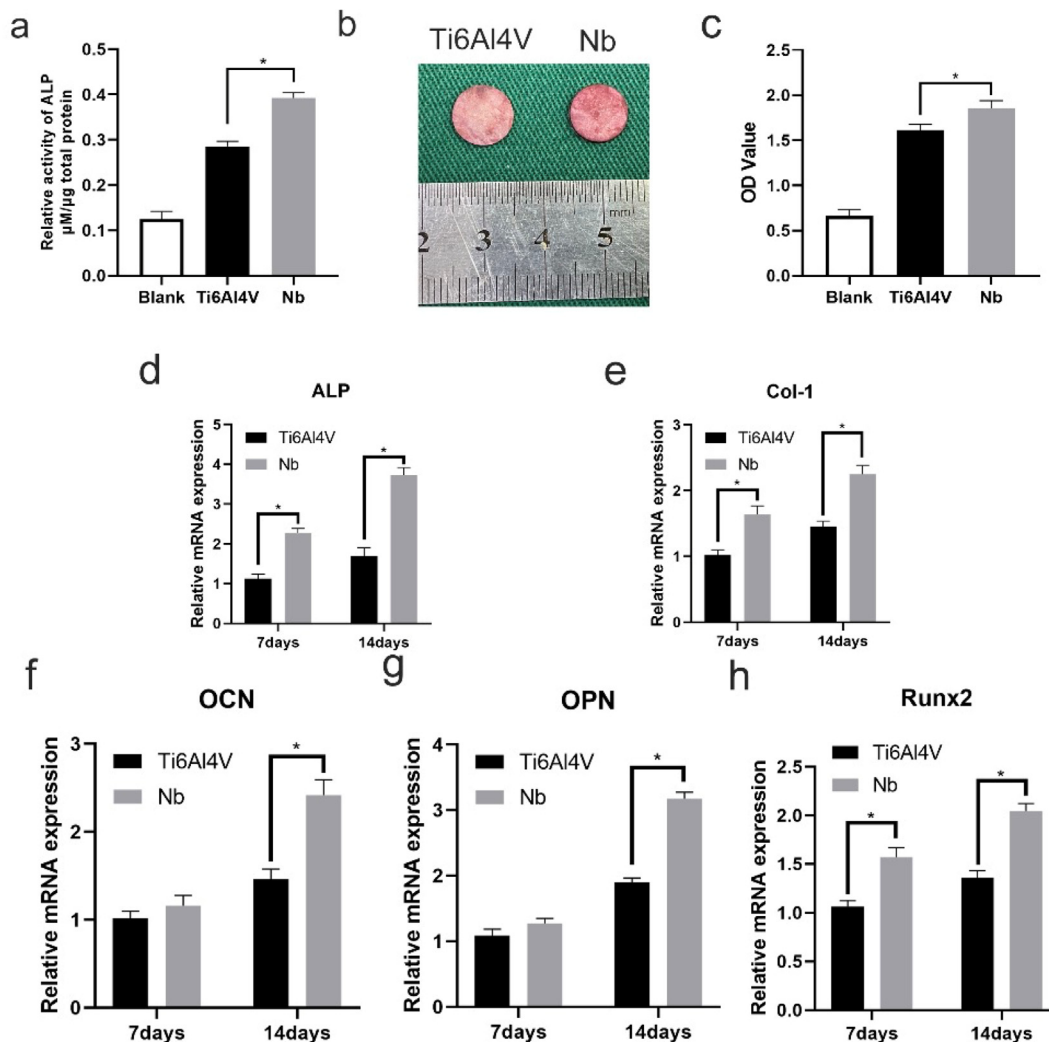


Figure 3. (a) Alkaline phosphatase (ALP) activity on day 7 and (c) semi-quantitative analysis of calcium nodules on day 21 of incubation on the discs, with high OD values indicating increased calcium nodule formation on the niobium (Nb) stent. (b) Alizarin red staining of the discs. Expression of osteogenesis-related genes: *ALP* (d), *Col-1* (e), *OCN* (f), *OPN* (g), *Runx2* (h) (n = 3/group). *P < 0.05, versus Ti6Al4V group).

calcein. The distance between calcein markers was used to represent the temporal change in new bone formation or bone remodelling. During the callus formation phase, a greater distance between calcein markers indicates faster bone formation. In this study, at weeks 4 and 8, the greater distance between calcein markers in the Nb group compared with that in the Ti6Al4V group indicated that Nb induced new bone formation (Fig. S1). At week 12, the distance between calcein markers decreased in both groups, suggesting the occurrence of bone remodelling.

3.8. Transcriptomic analysis

To determine the effect of Nb on fracture healing, a transcriptomic analysis was conducted. 1676 differentially expressed genes (a threshold with absolute log₂ fold-change >1 and p < 0.05) were identified. GO analysis revealed that these differentially expressed genes were associated with biological processes involved in fracture healing, such as the regulation of osteogenesis, angiogenesis, and other processes (Fig. 6a). An analysis of the bone development process indicated that related genes were induced (Fig. 6b). In addition, KEGG enrichment analysis showed that the PI3K-Akt signalling pathway was upregulated by Nb (Fig. 6c).

3.9. Immunohistochemical evaluation

Compared with the control group, the results of immunofluorescence staining at 4w and 8w showed that the expression in the callus of the Nb group was higher than that of the Ti6Al4V group (Fig. 7). This result suggests that Nb may activate the PI3K-Akt signalling pathway in the early stage of fracture healing.

3.10. Western blot analysis

The proteins expression of Akt, PI3K, Col-1, OCN, ALP and OPN was detected by protein blotting (Fig. 8a). The grayscale values of the protein bands were determined. Statistics were then used from the grayscale values/internal parameters. The results have confirmed the role of Nb in promoting the expression of osteogenic-related proteins (Fig. 8b,c,d,e) and upregulating the PI3K-Akt signalling pathway (Fig. 8f,g,h,i).

3.11. Biosafety evaluation

No significant differences were observed between the body weights of animals in the Nb and Ti6Al4V groups (Fig. S2a). The visceral organs,

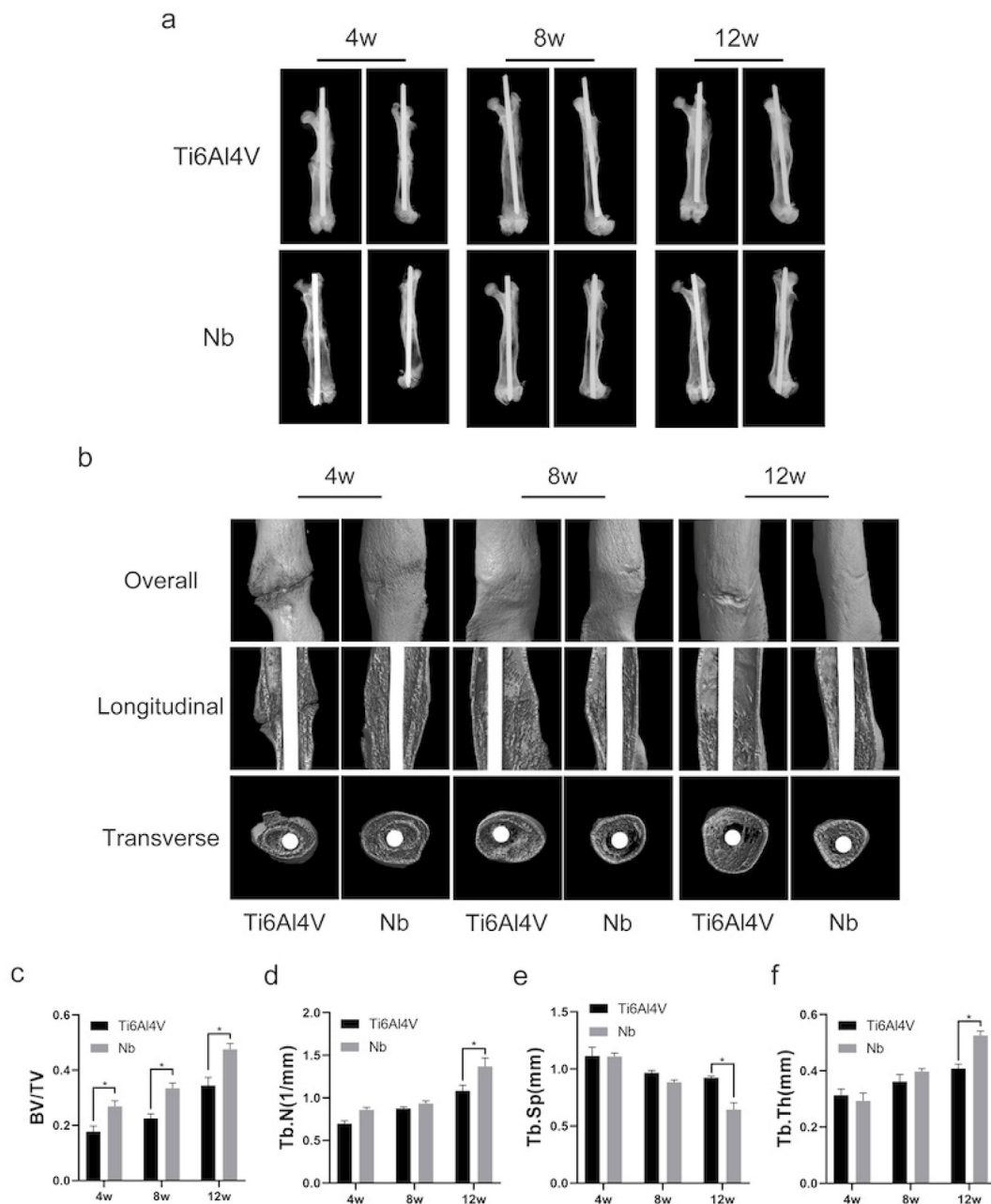


Figure 4. (a) X-ray follow-up image (front and side view). (b) Micro-CT images of the femoral specimen. (c) Bone volume fraction (BV/TV), (d) Trabecular number (Tb.N), (e) trabecular spacing (Tb.Sp), and (f) trabecular thickness (Tb.Th) of the niobium (Nb) and Ti6Al4V groups at 4, 8, and 12 weeks after implantation (n = 3/group). *P < 0.05, versus Ti6Al4V group).

including the liver, spleen, and kidney, were collected at the end of the experiment for histological analysis. The histological microstructure of the viscera was observed by organ HE staining using light microscopy, and no microscopic differences in the microstructure of the heart, liver, spleen, lungs, or kidneys were found between the Nb and Ti6Al4V groups (Fig. S2b).

4. Discussion

Human bone is a complex organ with multiple functions, including haematopoiesis, regulation and storage of critical minerals, protection of vital organs, and facilitation of movement. The present study first evaluated the biocompatibility and osteogenic differentiation activity of Nb metal via *in vitro* experiments, of which the experimental results suggested that Nb demonstrates superior biocompatibility and osteogenic effects

than Ti6Al4V, indicating that Nb has the enhanced biocompatibility required for clinical applications. Next, we utilized Nb metal as an intramedullary nail in a rat femur fracture model to investigate the effect of Nb on fracture healing, with the most commonly used material Ti6Al4V as a control group. Our *in vivo* experimental results have confirmed that Nb metal intramedullary nails can reduce the fracture healing time by promoting early fracture callus formation. Thus, Nb-based plates can be an effective means for fracture treatments in clinical practice and have good clinical translation prospects.

Currently, internal fixation devices widely used in clinical practice are mainly made of stainless steel and Ti alloys. However, these rigid bone implant materials have many insurmountable disadvantages, such as stress shielding, inactivity [17], and implant infection [18]. Driven by such clinical needs, the development of implant materials for hard tissues is focused on optimising and improving its mechanical and

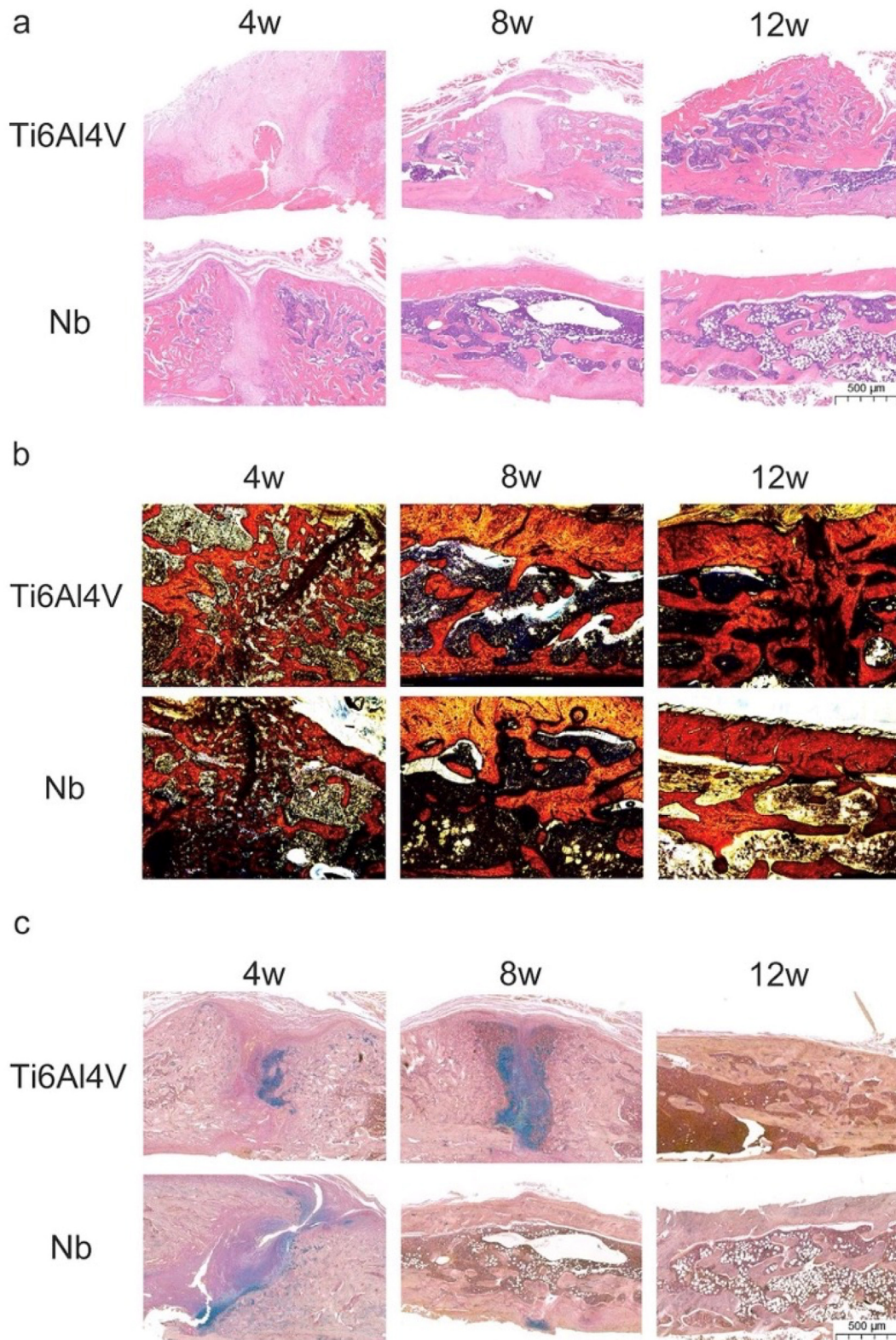


Figure 5. (a) Staining of the fracture using HE staining. (b) Assessment of fracture repair using van Gieson staining. (c) Calcification of bone and cartilage at the callus site was assessed using Movat staining.

biocompatibility properties. Currently, bionic coatings are used to modify implant surfaces to enhance the bioactivity of implants and resist infection, thereby extending the life of implants and reducing the risk of secondary surgical revisions. Hydroxyapatite (HAp), which has excellent osteoconductivity, bioactivity, and the ability to form strong

bone-calcium phosphate interfaces, is an ideal alternative [19]. Compared with uncoated devices, HAp-coated implants exhibit a longer post-implantation life and proved to be particularly beneficial for younger patients [20]. However, the main problem remains the weak adhesion between the HAp coating and the underlying substrate, which

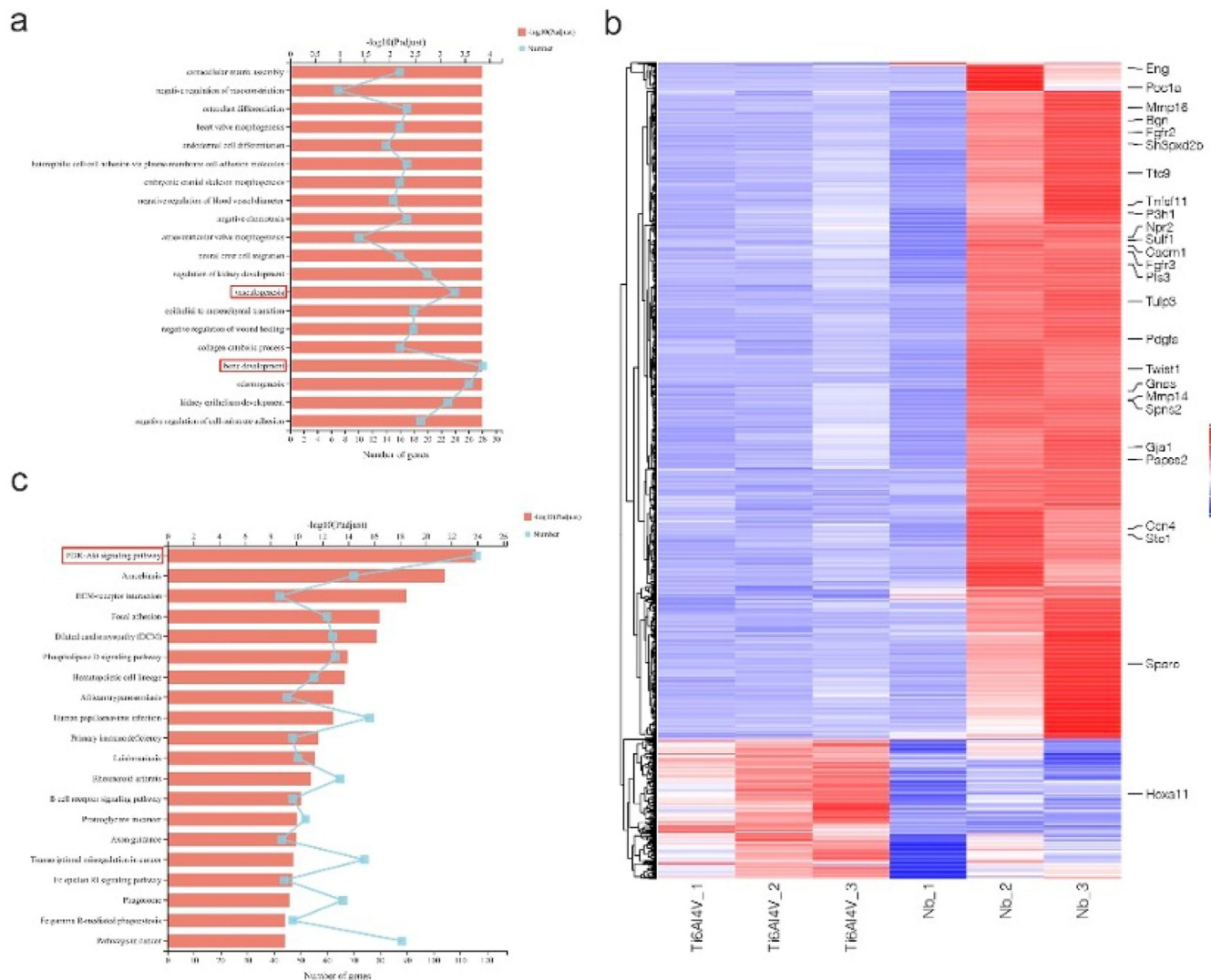


Figure 6. Transcriptomic analysis of callus tissues at week 8. (a) Gene Ontology (GO) enrichment analysis of differentially expressed genes in callus tissue. (b) Differentially expressed genes in the GO terms of the bone development process. (c) Kyoto Encyclopedia of Genes and Genomes (KEGG) enrichment analysis of the PI3K-Akt signalling pathway.

can lead to delamination [21], and particles from the delamination of the coating can cause an inflammatory response [22].

In addition to increasing the coatings of implants, methods for optimising include the development of new implant materials as well, such as Ta metal and its alloys. Ta exhibits excellent chemical stability and good biocompatibility as Ti. However, owing to its high elasticity modulus and weight, the clinical application of Ta is greatly limited. Therefore, many studies have attempted to find various ways to prepare Ta metallic materials with suitable mechanical properties. For example, porous structures are formed to reduce the weight and elastic modulus of Ta for dental and orthopaedic applications, as materials for bone defect repair [23]. Furthermore, porous Ta has been developed for intrasosseous growth applications, such as hip and knee replacements and spinal surgery, etc [24]. As a new implant, porous Ta has the features of good biocompatibility, excellent bioactivity, good corrosion resistance, and suitable biomechanical properties. So far, a number of basic and clinical studies have reported on Ta. As is reported, Ta-related products have been used in clinical practice [25], though there are still some limitations of Ta to be overcome. Due to the inconsistency of parameters in the various types of Ta-containing implants, there is no uniform optimisation of parameters. Although many studies have been conducted on Ti-Ta alloys, the optimal ratio of Ti-Ta content has not yet been determined,

and new material modification methods need to be developed. And owing to the high atomic weight and high X-ray absorption of Ta, it is difficult to obtain perfect imaging results to demonstrate the osteogenic activity and inward growth of Ta implants via standard imaging evaluation techniques [26].

Nb proved to have very similar physical and chemical properties to Ta and are widely sought after for their excellent biocompatibility, mechanical properties, corrosion resistance, and osteoconductivity. A large quantities of studies have been conducted on Nb-based coatings; for example, previous research has indicated that Nb₂O₅ is commonly used as a protective and osteogenic coating for Ti alloys and stainless steels to improve the biocompatibility and corrosion resistance of implants [27]. NbC films can promote cell attachment, mineralisation, and osteogenic differentiation, showing optimal protection efficiency and osteogenic potential [11]. In addition, PEEK/Nb₂O₅ composites exhibit a sub-microstructure surface induced by Nb₂O₅, and its surface roughness, hydrophilicity, surface energy, and protein adsorption of rise significantly as the Nb increases, promoting BMSC adhesion and proliferation, as well as osteogenic differentiation [16]. The use of Nb alloys are now attracting attention for use in stents, and studies have shown that porous Ti-25Nb alloys show good biocompatibility, and the experiments of cell adhesion and proliferation have indicated good cell growth results on the

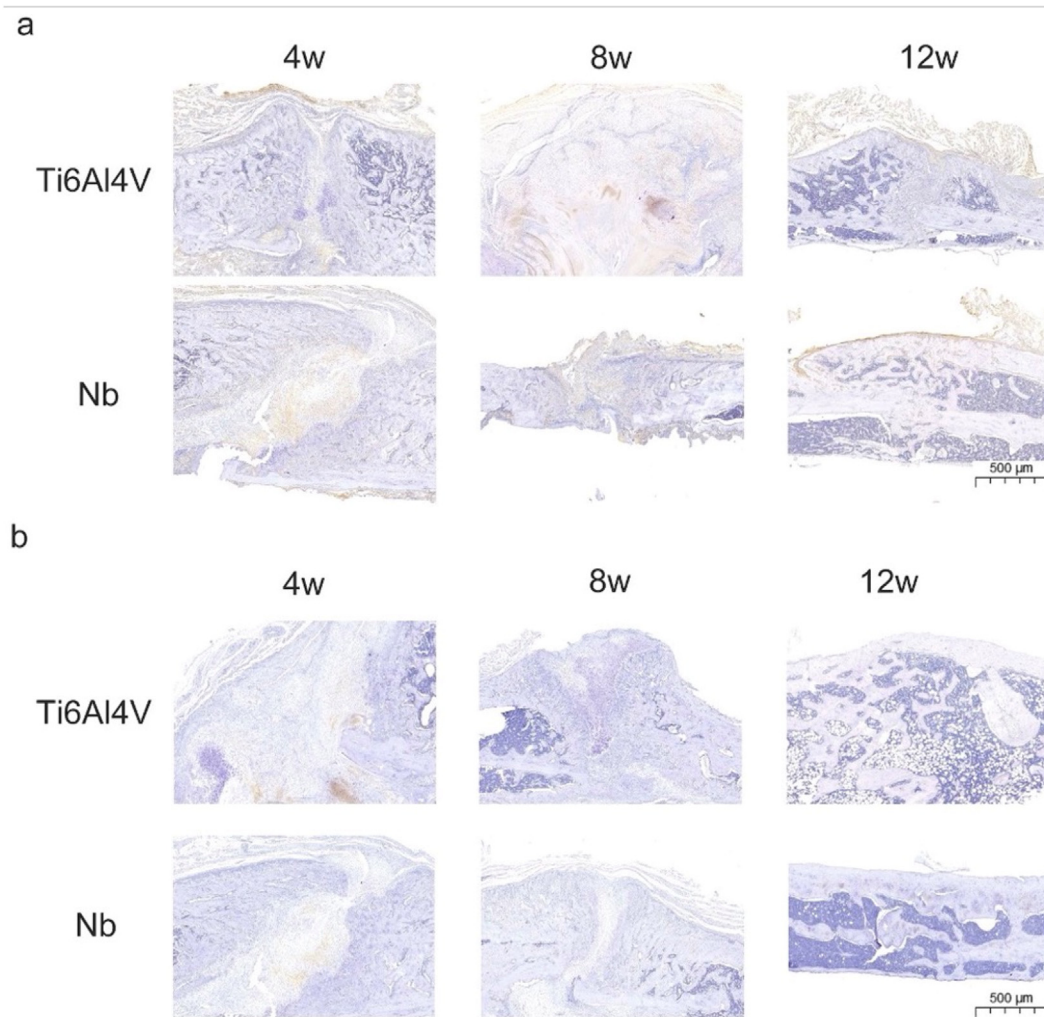


Figure 7. Immunohistochemical staining for PI3K (a) and Akt (b).

alloy surface and within the pores without causing significant inflammatory responses [28]. In the present study, Nb proved to promote MC3T3-E1 cell attachment and osteogenic differentiation compared to those with Ti6Al4V with better osteogenic potential, which is consistent with previous studies [9]. Subsequently, we performed *in vivo* studies to determine the effect of Nb on osteogenesis. In imaging and histological experiments, the Nb group was confirmed to exhibit earlier callus formation at week 4 than the Ti6Al4V group through observation, and the Nb group showed better remodelling of the callus tissue than the Ti6Al4V group at week 8. Moreover, at week 12, callus remodelling was also completed faster in the Nb group than in the control group, indicating that Nb can accelerate fracture healing.

There are many important signalling pathways involved in fracture healing and repair, such as Wnt/ β -catenin, Notch, bone morphogenetic protein (BMP)/TGF- β , and platelet-derived growth factor (PDGF). Wnt signalling, which regulates a wide range of cell processes associated with osteogenesis, is thought to be involved in the overall healing process. And it is significantly induced in fracture healing via canonical β -catenin Wnt signalling, indicating its osteoconductive role [29]. Activation of the Wnt/ β -catenin signalling pathway results in accelerated osteoblast proliferation and differentiation, leading to a significant increase in bone mass in the Axin2-knockout mouse model [30]. The Notch signalling pathway, a highly evolutionarily conserved ligand-receptor signalling pathway, plays an essential role in cell survival, proliferation, differentiation, developmental processes, and homeostasis *in vivo* [31]. Various studies based on mouse models have shown that inhibition of the Notch

signalling pathway in bone progenitor cells leads to a reduction in bone marrow-derived mesenchymal stem cells [32]. BMPs, as multifunctional paracrine growth factors, belong to the transforming growth factor β (TGF β) superfamily and play an important role in osteogenesis. And they are vital in osteogenesis. Both *in vivo* and *in vitro* experiments have demonstrated that the BMP/TGF- β signalling pathway is essential at the onset of skeletogenesis [33]. Furthermore, BMP signalling is critical for osteogenesis progression and maturation, which might depend on the transcription factor Osterix acting downstream of Runx2 [34]. PDGF, an extracellular factor, are important in regulating numerous cellular functions in the skeleton by increasing the number of MSCs through its mitogenic, angiogenic, and proliferative activities [35]. The increase in bone regeneration is achieved through two major PDGF-mediated mechanisms. First, it increases the number of bone marrow MSCs, which then differentiate into osteoblasts. Second, a more important mechanism is the chemotaxis and activation of macrophages [36]. Thus, to search for mechanisms related to the acceleration of fracture healing mediated by Nb, we extracted RNA from callus tissue at week 8 for genome sequencing. Transcriptomic analysis has revealed that the PI3K-Akt signalling pathway was upregulated in the Nb group.

The PI3K-Akt signalling pathway, which lies the foundation in a variety of cellular processes including cell growth, survival, proliferation, and motility, is one of the key pathways regulating cellular behaviours, including apoptosis, proliferation, and differentiation. And it is frequently activated in a variety of human cancers [37]. PI3K phosphorylates PIP₂ to form PIP₃, which acts as a second messenger to

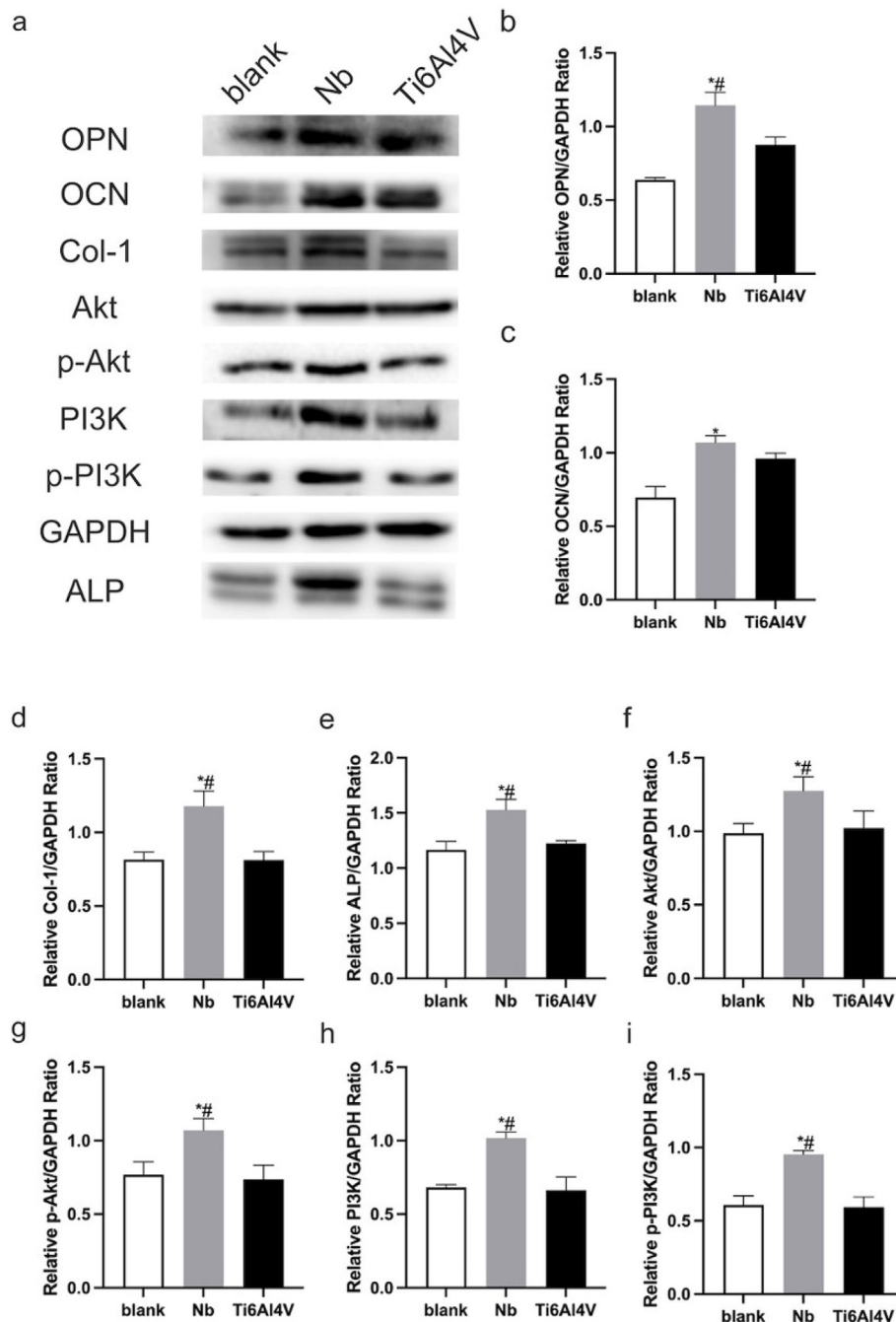


Figure 8. Western blot results suggest that the promotion of fracture healing by niobium (Nb) might be related to the expression of PI3K-Akt signalling pathway components (n = 3/group. *P < 0.05, versus blank group , #P < 0.05, versus Ti6Al4V group).

activate the serine/threonine kinase AKT (also known as protein kinase B) [38]. Activated AKT phosphorylates many downstream substrates that are involved in the regulation of cell survival, apoptosis, proliferation, protein synthesis, and other processes. These substrates are involved in regulating cell survival, apoptosis, proliferation, protein synthesis, and other processes. Many have reported on the key regulatory functions of PI3K signalling and its downstream targets in bone formation and remodelling. Liu et al. [39] demonstrated that MiR-21 promotes fracture healing in rats through the activation of PI3K-Akt signalling pathway. Dong et al. [40] found that the β -catenin transcriptional activity inhibitor ICG001 attenuates PI3K-Akt-induced osteoblast proliferation, differentiation, and mineralisation, revealing the existence of Wnt/PI3K/AKT/ β -catenin signalling relationships in osteoblasts and suggesting

that PI3K-Akt and Wnt/ β -catenin pathways are closely related to fracture healing. According to Xing et al. [41], Dexamethasone (Dex) was found to simultaneously inhibit the phosphorylation of protein kinase B (Akt) and the expression level of Sema3A in BMSCs, which inhibits osteoblast differentiation by inhibiting the expression of Sema3A through the PI3K/Akt pathway. Zhang et al. [42] have proved that exosomes could enhance the osteogenic inductive ability of β -TCP by activating the PI3K/Akt signaling pathway of hBMSCs. In addition, some signalling pathways exert their osteogenic effects by targeting the PI3K-Akt signalling pathway. For example, bFGF can promote the expression of OPG, Runx2, p-Akt, and BMP-2 proteins through the activated PI3K-Akt signalling pathway, as well as the proliferation, differentiation, and osteogenesis of osteoblasts on the Ti surface [43]. We observed higher

expression of PI3K and Akt in the Nb group at weeks 4 and 8, via histological staining, and significantly at the callus, suggesting a role in endochondral ossification of the callus. Endochondral ossification is an important process in fracture healing [29], which is induced by BMPs, TGF- β 2, and TGF- β 3 signalling in healing cartilage tissue [44]. At the end of this phase, the synthesised cartilage calcifies and are replaced by woven bone. Studies have shown that BMP-4 induces Akt phosphorylation [45]. We thus speculate that the mechanism by which Nb promotes fracture healing is likely through the induction of Akt phosphorylation by BMP and upregulation of the PI3K-Akt signalling pathway. Thus, we suggest that Nb might promote osteoblast function and thus accelerate fracture healing by upregulating PI3K-Akt signalling. However, we still need to understand how these signalling pathways are interrelated to gain a clearer understanding of the mechanisms underlying the effects of Nb on fracture healing.

PI3K-Akt signalling also works in osteoclast activation. It was found in Ma et al.'s study [46] that Trpv6 inhibits osteoclastogenesis by reducing the phosphoprotein or total protein ratio in the IGF-PI3K-AKT signaling pathway. The active stage of osteoclasts is mainly in the early hematoma stage and the late callus remodeling stage [47], but the transcriptomic analysis was done in the stage of endochondral ossification. Therefore, we did not pay much attention to the effect of PI3K-Akt signaling pathway on osteoclasts. Through *ex vivo* experiments, we have found that Nb can regulate PI3K-Akt signalling, yet our study still has some limitations: (1) we did not test the mechanical properties of the samples, although we believe that the efficacy of the Nb group in promoting fracture healing has been confirmed by X-ray, Micro-CT and histochemistry results; (2) there is a lack of in-depth studies on the PI3K-Akt signaling pathway upstream and downstream mechanisms, which will be the next focus to consider in the future.

5. Conclusions

In the present study, the biocompatibility, osseointegration and osteogenic properties of Nb metal were evaluated. *In vitro* studies have indicated that Nb can promote cell proliferation, adhesion, and osteogenic differentiation compared to those with Ti6Al4V. In addition, X-ray and micro-CT results of Nb group have demonstrated its excellency in fracture healing compared with that in the control group at the same time points. Histological analysis showed that the Nb group had better callus remodelling than the Ti6Al4V group. We also found that Nb might promote fracture healing by affecting the PI3K-Akt pathway in fracture healing and thus promoting fracture healing. Furthermore, it is found that Nb metal implants did not cause any local or systemic toxicity to major organs. Although it remains to be further investigated whether the action of Nb in human is consistent with that in mice as presented in the present study, our results have confirmed that Nb metal implants have potential for future orthopaedic applications.

Funding support statement

This work was supported by the National Natural Science Foundation of China [grant number 81972058, 81902194]; the Science and Technology Commission of Shanghai Municipality [grant number 22YF1422900]; the Shanghai Municipal Key Clinical Specialty, China [grant number shslczdzk06701]; the National Facility for Translational Medicine (Shanghai), China [grant number TMSZ-2020-207]; the Shanghai Engineering Research Center of orthopedic innovative instruments and personalized medicine instruments and personalized medicine [grant number 19DZ2250200]; and Key R&D Programs of Ningxia, China [grant number: 2020BCH01001].

Author contributions

The first three authors (Jia Tan, Jiixin Li, Bojun Cao) contributed equally to this manuscript. Jia Tan: Conceptualization, Investigation,

Formal analysis, Writing—original draft. Jiixin Li: Investigation, Formal analysis, Writing – original draft. Bojun Cao: Investigation, Formal analysis. Junxiang Wu: Investigation, Formal analysis. Dinghao Luo: Formal analysis. Zhaoyang Ran: Formal analysis. Liang Deng: Methodology. Xiaoping Li: Methodology. Wenbo Jiang: Methodology. Kai Xie: Conceptualization, Methodology, Supervision, Writing—review & editing. Lei Wang: Methodology, Supervision, Writing—review & editing. Yongqiang Hao: Conceptualization, Supervision, Funding acquisition, Writing – review & editing.

Declaration of competing interest

The authors have no conflicts of interest relevant to this article.

Acknowledgements

We would like to thank Ningxia Orient Ta Ind Co for providing the Niobium sheet and stick.

Appendix A. Supplementary data

Supplementary data to this article can be found online at <https://doi.org/10.1016/j.jot.2022.08.007>.

References

- [1] Liu X, McKenzie JA, Maschhoff CW, Gardner MJ, Silva MJ. Exogenous hedgehog antagonist delays but does not prevent fracture healing in young mice. *Bone* 2017; 103:241–51.
- [2] Wang L, Li G, Ren L, Kong X, Wang Y, Han X, et al. Nano-copper-bearing stainless steel promotes fracture healing by accelerating the callus evolution process. *Int J Nanomed* 2017;12:8443–57.
- [3] Tian L, Tang N, Ngai T, Wu C, Ruan Y, Huang L, et al. Hybrid fracture fixation systems developed for orthopaedic applications: a general review. *J Orthop Translat* 2019;16:1–13.
- [4] Xie K, Zhou Z, Guo Y, Wang L, Li G, Zhao S, et al. Long-term prevention of bacterial infection and enhanced osteoinductivity of a hybrid coating with selective silver toxicity. *Adv Healthc Mater* 2019;8(5):e1801465.
- [5] Xie K, Wang L, Guo Y, Zhao S, Yang Y, Dong D, et al. Effectiveness and safety of biodegradable Mg-Nd-Zn-Zr alloy screws for the treatment of medial malleolar fractures. *J Orthop Translat* 2021;27:96–100.
- [6] Pajarinen J, Lin T, Gibon E, Kohno Y, Maruyama M, Nathan K, et al. Mesenchymal stem cell-macrophage crosstalk and bone healing. *Biomaterials* 2019;196:80–9.
- [7] Guo Y, Xie K, Jiang W, Wang L, Li G, Zhao S, et al. In vitro and in vivo study of 3D-printed porous tantalum scaffolds for repairing bone defects. *ACS Biomater Sci Eng* 2018;5(2):1123–33.
- [8] Li G, Wang L, Pan W, Yang F, Jiang W, Wu X, et al. In vitro and in vivo study of additive manufactured porous Ti6Al4V scaffolds for repairing bone defects. *Sci Rep* 2016;6:34072.
- [9] Matsuno H, Yokoyama A, Watari F, Uo M, Kawasaki T. Biocompatibility and osteogenesis of refractory metal implants, titanium, hafnium, niobium, tantalum and rhenium. *Biomaterials* 2001;22(11):1253–62.
- [10] Bartolome JF, Moya JS, Couceiro R, Gutierrez-Gonzalez CF, Guitian F, Martinez-Insua A. In vitro and in vivo evaluation of a new zirconia/niobium biocermet for hard tissue replacement. *Biomaterials* 2016;76:313–20.
- [11] Xu Z, Yate L, Qiu Y, Aperador W, Coy E, Jiang B, et al. Potential of niobium-based thin films as a protective and osteogenic coating for dental implants: the role of the nonmetal elements. *Mater Sci Eng C Mater Biol Appl* 2019;96:166–75.
- [12] Wang XJ, Li YC, Lin JG, Yamada Y, Hodgson PD, Wen CE. In vitro bioactivity evaluation of titanium and niobium metals with different surface morphologies. *Acta Biomater* 2008;4(5):1530–5.
- [13] Vandrovceva M, Jirka I, Novotna K, Lisa V, Frank O, Kolska Z, et al. Interaction of human osteoblast-like Saos-2 and MG-63 cells with thermally oxidized surfaces of a titanium-niobium alloy. *PLoS One* 2014;9(6):e100475.
- [14] Velten Eisenbarth, Schanne Brems. Biocompatible Nb2O5 thin films prepared by means of the sol-gel process. *J Mater Sci Mater Med* 2004;15:457–61.
- [15] Mazur M, Kalisz M, Wojcieszak D, Grobelny M, Mazur P, Kaczmarek D, et al. Determination of structural, mechanical and corrosion properties of Nb2O5 and (NbCu 1-y)Ox thin films deposited on Ti6Al4V alloy substrates for dental implant applications. *Mater Sci Eng C Mater Biol Appl* 2015;47:211–21.
- [16] Ge J, Wang F, Xu Z, Shen X, Gao C, Wang D, et al. Influences of niobium pentoxide on roughness, hydrophilicity, surface energy and protein absorption, and cellular responses to PEEK based composites for orthopedic applications. *J Mater Chem B* 2020;8(13):2618–26.
- [17] Hayes JS, Richards RG. The use of titanium and stainless steel in fracture fixation. *Expert Rev Med Dev* 2010;7(6):843–53.
- [18] Darouiche RO. Treatment of infections associated with surgical implants. *N Engl J Med* 2004;172(5):2102–02.

- [19] LeGeros Zapanta R. Properties of osteoconductive biomaterials: calcium phosphates. *Clin Orthop Relat Res* 2002;395:81–98.
- [20] Best SM, Porter AE, Thian ES, Huang J. Bioceramics: past, present and for the future. *J Eur Ceram Soc* 2008;28(7):1319–27.
- [21] Kweh S, Khor KA, Cheang P. An in vitro investigation of plasma sprayed hydroxyapatite (HA) coatings produced with flame-spheroidized feedstock. *Biomaterials* 2002;23(3):775–85.
- [22] Ramaswamy Y, Wu C, Zreiqat H. Orthopedic coating materials: considerations and applications. *Expet Rev Med Dev* 2009;6(4):423–30.
- [23] Levine BR, Sporer S, Poggie RA, Della Valle CJ, Jacobs JJ. Experimental and clinical performance of porous tantalum in orthopedic surgery. *Biomaterials* 2006;27(27):4671–81.
- [24] Bobyn JD, Poggie PA, Krygier JJ, Lewallen DG, Hanssen AD, Lewis RJ, et al. Clinical validation of a structural porous tantalum biomaterial for adult reconstruction. *Journal of Bone & Joint Surgery American* 2004;86(suppl 2):123. A Suppl 2.
- [25] DeFrancesco CJ, Canseco JA, Nelson CL, Israelite CL, Kamath AF. Uncemented tantalum monoblock tibial fixation for total knee arthroplasty in patients less than 60 Years of age: mean 10-year follow-up. *J Bone Joint Surg Am* 2018;100(10):865–70.
- [26] Qian H, Lei T, Lei P, Hu Y. Additively manufactured tantalum implants for repairing bone defects: a systematic review. *Tissue Eng B Rev* 2021;27(2):166–80.
- [27] Ramírez G, Rodil SE, Arzate H, Muhl S, Olaya JJ. Niobium based coatings for dental implants. *Appl Surf Sci* 2011;257(7):2555–9.
- [28] Xu J, Weng XJ, Wang X, Huang JZ, Zhang C, Muhammad H, et al. Potential use of porous titanium-niobium alloy in orthopedic implants: preparation and experimental study of its biocompatibility in vitro. *PLoS One* 2013;8(11):e79289.
- [29] Majidinia M, Sadeghpour A, Yousefi B. The roles of signaling pathways in bone repair and regeneration. *J Cell Physiol* 2018;233(4):2937–48.
- [30] Yan Y, Tang D, Chen M, Huang J, Xie R, Jonason JH, et al. Axin2 controls bone remodeling through the beta-catenin-BMP signaling pathway in adult mice. *J Cell Sci* 2009;122(Pt 19):3566–78.
- [31] Majidinia M, Alizadeh E, Yousefi B, Akbarzadeh M, Zarghami N. Downregulation of Notch signaling pathway as an effective chemosensitizer for cancer treatment. *Drug Res* 2016;66(11):571–9.
- [32] Hilton MJ, Tu X, Wu X, Bai S, Zhao H, Kobayashi T, et al. Notch signaling maintains bone marrow mesenchymal progenitors by suppressing osteoblast differentiation. *Nat Med* 2008;14(3):306–14.
- [33] Deschaseaux F, Sensebe L, Heymann D. Mechanisms of bone repair and regeneration. *Trends Mol Med* 2009;15(9):417–29.
- [34] Nakashima K, Xin Z, Kunkel G, Zhang Z, Jian M, Behringer RR, et al. The novel zinc finger-containing transcription factor osterix is required for osteoblast differentiation and bone formation. *Cell* 2002;108(1):17–29.
- [35] Kaigler D, Avila G, Wisner-Lynch L, Nevins ML, Nevins M, Rasperini G, et al. Platelet-derived growth factor applications in periodontal and peri-implant bone regeneration. *Expet Opin Biol Ther* 2011;11(3):375.
- [36] Prasun Shah, Louis Keppler, James Rutkowski. A review of Platelet Derived Growth Factor playing pivotal role in bone regeneration. *J Oral Implantol* 2014 Jun;40(3):330–40.
- [37] Chalhoub N, Baker SJ. PTEN and the PI3-kinase pathway in cancer. *Annu Rev Pathol* 2009;4:127–50.
- [38] Georgescu MM. PTEN tumor suppressor network in PI3K-Akt pathway control. *Genes Cancer* 2010;1(12):1170–7.
- [39] Liu Y, Liu J, Xia T, Mi BB, Liu GH. MiR-21 promotes fracture healing by activating the PI3K/Akt signaling pathway. *Eur Rev Med Pharmacol Sci* 2019 Apr;23(7):2727–33.
- [40] Dong J, Xu X, Zhang Q, Yuan Z, Tan B. The PI3K/AKT pathway promotes fracture healing through its crosstalk with Wnt/beta-catenin. *Exp Cell Res* 2020;394(1):112137.
- [41] Xing Q, Feng J, Zhang X. Glucocorticoids suppressed osteoblast differentiation by decreasing Sema3A expression via the PIK3/Akt pathway. *Exp Cell Res* 2021;403(1):112595.
- [42] Zhang J, Liu X, Li H, Chen C, Hu B, Niu X, et al. Exosomes/tricalcium phosphate combination scaffolds can enhance bone regeneration by activating the PI3K/Akt signaling pathway. *Stem Cell Res Ther* 2016;7(1):136.
- [43] Zheng AQ, Xiao J, Xie J, Lu PP, Ding X. bFGF enhances activation of osteoblast differentiation and osteogenesis on titanium surfaces via PI3K/Akt signaling pathway. *Int J Clin Exp Pathol* 2016;9(4):4680–92.
- [44] Tae-Joon Cho, Louis C, Gerstenfeld Thomas, et al. Differential temporal expression of members of the transforming growth factor β superfamily during murine fracture healing. *J Bone Miner Res* 2002 Mar;17(3):513–20.
- [45] Lee MY, Lim HW, Lee SH, Han HJ. Smad, PI3K/Akt, and Wnt-dependent signaling pathways are involved in BMP-4-induced ESC self-renewal. *Stem Cell* 2009;27(8):1858–68.
- [46] Ma J, Zhu L, Zhou Z, Song T, Yang L, Yan X, et al. The calcium channel TRPV6 is a novel regulator of RANKL-induced osteoclastic differentiation and bone absorption activity through the IGF-PI3K-AKT pathway. *Cell Prolif* 2021;54(1):e12955.
- [47] Wang T, Zhang X, Bikle DD. Osteogenic differentiation of periosteal cells during fracture healing. *J Cell Physiol* 2017;232(5):913–21.